Emerging Microbes & Infections
2025, VOL. 14, 2477639 (19 pages)
https://doi.org/10.1080/22221751.2025.2477639

Mpox virus poxin-schlafen fusion protein suppresses innate antiviral response by sequestering STAT2

Pearl Chan *, Zi-Wei Ye *, Wenlong Zhao, Chon-Phin Ong, Xiao-Yu Sun, Pak-Hin Hinson Cheung and Dong-Yan Jin

School of Biomedical Sciences, The University of Hong Kong, Pokfulam, Hong Kong

ABSTRACT

Mpox virus (MPXV) has to establish efficient interferon (IFN) antagonism for effective replication. MPXV-encoded IFN antagonists have not been fully elucidated. In this study, the IFN antagonism of poxin-schlafen (PoxS) fusion gene of MPXV was characterized. MPXV PoxS was capable of decreasing cGAS-produced 2′3′-cGAMP, like its ortholog poxin of vaccinia virus, which is the first known cytosolic nuclease that hydrolyses the 3′-5′ bond of 2′3′-cyclic GMP-AMP (cGAMP). However, MPXV PoxS did not suppress cGAS-STING-mediated type I IFN production. Instead, MPXV PoxS antagonized basal and type I IFN-induced expression of IFN-stimulated genes such as OAS1, SAMD9, SAMD9L, ISG15, ISG56 and IFIT3. Consistently, MPXV PoxS inhibited both basal and type I IFN-stimulated activity of interferon-stimulated response elements, but did not affect activation of IFN-γ-activated sites. Mechanistically, MPXV PoxS interacted with STAT2 and sequestered it in the cytoplasm. Both the viral schlafen fusion and the active site of 2′3′-cGAMP nuclease were required for STAT2 sequestration and consequent suppression of IFN-stimulated gene expression. MPXV PoxS conferred resistance to the suppression of MPXV replication by type I IFN. Taken together, our findings suggested that MPXV PoxS counteracts host antiviral response by sequestering STAT2 to circumvent basal and type I IFN-induced expression of antiviral genes.

ARTICLE HISTORY Received 25 October 2024; Revised 3 March 2025; Accepted 5 March 2025

KEYWORDS mpox virus; monkeypox virus; poxin; cGAS; STING; innate antiviral response; 2′3′-cGAMP hydrolase; STAT2

Introduction

Mpox (monkeypox) virus (MPXV) is the second most pathogenic orthopoxvirus that infects humans under the family of *Poxviridae* after variola virus, which was eradicated in the 1980s due to the success of smallpox vaccination with vaccinia virus [1,2]. With a broader host infectivity range, MPXV was not eradicated but persisted in natural reservoirs and secondary hosts, which might respectively be rodents and primates found in central and western Africa [3]. Since the 1980s during which global mandatory smallpox vaccination campaign was ceased, the frequency of MPXV infection in humans has increased substantially [4]. Unlike variola virus, human infection with MPXV was mostly evidenced with zoonotic transmission by direct contact with infected animals. Human-to-human transmission of mpox is rarely recorded until the recent outbreaks of mpox clade II since 2022, which has rapidly spread to more than 120 countries around the world [5]. The ongoing outbreaks of mpox clade I in the Democratic Republic of Congo and neighbouring countries are more concerning due to high mortality and altered epidemiological patterns [6]. As of February 2025, mpox of clades I and II affected more than 120,000 people and caused more than 270 deaths. It is now known that MPXV can effectively spread in human population mainly through direct contact with lesion and probably sexual transmission [7]. Respiratory droplet transmission of MPXV is not evidenced in humans despite being demonstrated in model animals such as Prairie dogs [8]. The success of MPXV in establishing effective infection, transmission and pathogenesis in humans raises new research questions that require more efforts to identify and characterize key viral factors that subvert host defence.

Type I interferon (IFN) response is a conserved and universal antiviral mechanism in mammals [9]. Orthopoxviruses must express multiple factors to establish IFN antagonism for effective replication in mammalian cells, as exemplified with vaccinia virus [10]. In contrast, modified vaccinia virus Ankara

CONTACT Pak-Hin Hinson Cheung hinson01@connect.hku.hk School of Biomedical Sciences, The University of Hong Kong, 21 Sassoon Road, Pokfulam, Hong Kong; Dong-Yan Jin dyjin@hku.hk School of Biomedical Sciences, The University of Hong Kong, 21 Sassoon Road, Pokfulam, Hong Kong
*These authors contributed equally to this work.

Supplemental data for this article can be accessed online at https://doi.org/10.1080/22221751.2025.2477639.

(MVA), which was derived from the extensive adaptation of the parental vaccinia virus in chicken embryonic fibroblasts, has lost IFN antagonism and is therefore unable to propagate in mammalian cells [11,12]. Whereas MPXV, vaccinia virus and other poxviruses share some common counter-defence mechanisms, MPXV also has its own and unique characteristics in IFN antagonism compared to vaccinia virus. Innate immune antagonists shared by MPXV, vaccinia virus and other poxviruses include C6, which inhibits TBK1, STAT2 and TRIM5α [13–15], and F17, which suppresses cGAS [16]. On the other hand, the well-known protein kinase R (PKR) suppressor E3L gene of vaccinia virus is truncated and non-functional in MPXV [17]. Reconstitution of the MPXV homologue, namely F3L, to E3L knockout vaccinia virus did not rescue IFN antagonism [17]. MPXV does not express K3L gene which is another essential PKR suppressor and type I IFN antagonist of vaccinia virus [18]. Instead, MPXV expresses G1R gene which potently suppresses NF-κB signalling but is truncated in vaccinia virus [19]. As such, MPXV expresses a unique set of IFN antagonists that shape its strain-specific pathogenicity and transmissibility in various mammalian hosts compared to other human-infecting orthopoxviruses [20,21]. Some of them may be important in determining the effective host range, pathogenicity and transmissibility of MPXV.

Vaccinia virus poxin was first characterized in 2019 to be a cytosolic nuclease that can specifically hydrolyse the 3′−5′ phosphodiester bond of 2′3′-cGAMP [22]. Poxin and its 2′3′-cGAMP nuclease activity was found to be conserved in baculoviruses, insects but only a subset of poxviruses including some of those in insects, rodents, and bats, suggestive of horizontal transfer of the poxin gene from insects or insect viruses [23,24]. In orthopoxviruses, poxin is expressed as an early gene either alone or in C-terminal fusion with the viral schlafen gene (vSlfn), which encodes an inhibitor of STING [25]. Poxin-vSlfn fusion protein (PoxS) is a marker of rodent-tropic orthopoxviruses, such as cowpox (CPXV), camelpox, Ectromelia virus (mousepox) and MPXV. In non-rodent-tropic orthopoxviruses such as vaccinia virus and horsepox virus, poxin is not fused with vSlfn. Interestingly, the expression of poxin is defective in variola virus and MVA, which have a very narrow non-rodent host range in humans and chickens, respectively.

2′3′-cGAMP is a well-known agonist of STING in the signalling pathway of type I IFN production [26]. Unlike ENPP1 which is a known 2′3′-cGAMP nuclease facing extracellular space and capable of suppressing cGAS-STING-mediated type I IFN production [27], the suppressive effect of poxin against cGAS and STING pathway is controversial. In two studies, deletion of PoxS of Ectromelia virus or poxin of vaccinia virus was found to strongly attenuate virus replication and IFN antagonism in mice [22,25]. However, in the same study for vaccinia virus, poxin knockout did not show attenuated IFN antagonism or replication in human A549 cells [22]. In another study, infection with poxin-deleted vaccinia virus produced similar IFN response in murine bone marrow-derived monocytes [28]. Finally, in a more recent study using oncolytic vaccinia virus, poxin deletion did not significantly promote type I IFN production in human cells or in mice [29]. Therefore, viral poxin might not exert a suppressive effect on cGAS-STING-mediated type I IFN production in all circumstances. It is noteworthy that poxviruses encode other suppressors of cGAS and STING including vaccinia virus E5 [28] and F17 [16] as well as myxoma virus M062 [30].

MPXV PoxS has intact 2′3′-cGAMP binding sites, nuclease active sites, and the ability to hydrolyse 3′−5′ phosphodiester bond *in vitro* [22,31]. In this study, we hypothesized that MPXV PoxS should reduce cGAS-STING-mediated type I IFN response by diminishing the pool of 2′3′-cGAMP for STING activation. To our surprise, although we found that MPXV PoxS expression reduced 2′3′-cGAMP produced by cGAS, MPXV PoxS can suppress neither 2′3′-cGAMP-STING- nor MVA-induced type I IFN production. Interestingly, we observed that MPXV PoxS significantly repressed IFN-stimulated gene (ISG) expression. We also found that MPXV PoxS suppressed the activity of interferon-stimulated response elements (ISRE) but not that of IFN-γ-activated sites (GAS). Furthermore, MPXV PoxS exclusively formed cytosolic clustering pattern in human cells, which disappeared upon removal of vSlfn fusion. In addition, MPXV PoxS clustered with STAT2 but not STAT1 or JAK1. Colocalization of MPXV PoxS and STAT2 required the intact active site of 2′3′-cGAMP nuclease. STAT2 still colocalized with MPXV PoxS mutant having no vSlfn. Finally, MPXV PoxS suppressed ISG expression and conferred IFNβ resistance during MPXV infection, which required vSlfn fusion and the intact active site of 2′3-cGAMP nuclease.

Materials and methods

Plasmids, 2′3′-cGAMP and human IFN recombinant proteins

Expression plasmid for MPXV PoxS was generated by ligating the purified PCR fragment of the MPXV PoxS gene of the MPXV isolate hMpxV/Hong Kong/HKU-220914-001/2022 with pcDNA-3.1A-V5/6xHis [32]. The OPG188 or the MPXV PoxS gene is 100% identical to that of the USA MA001 strain (Figure 1). The

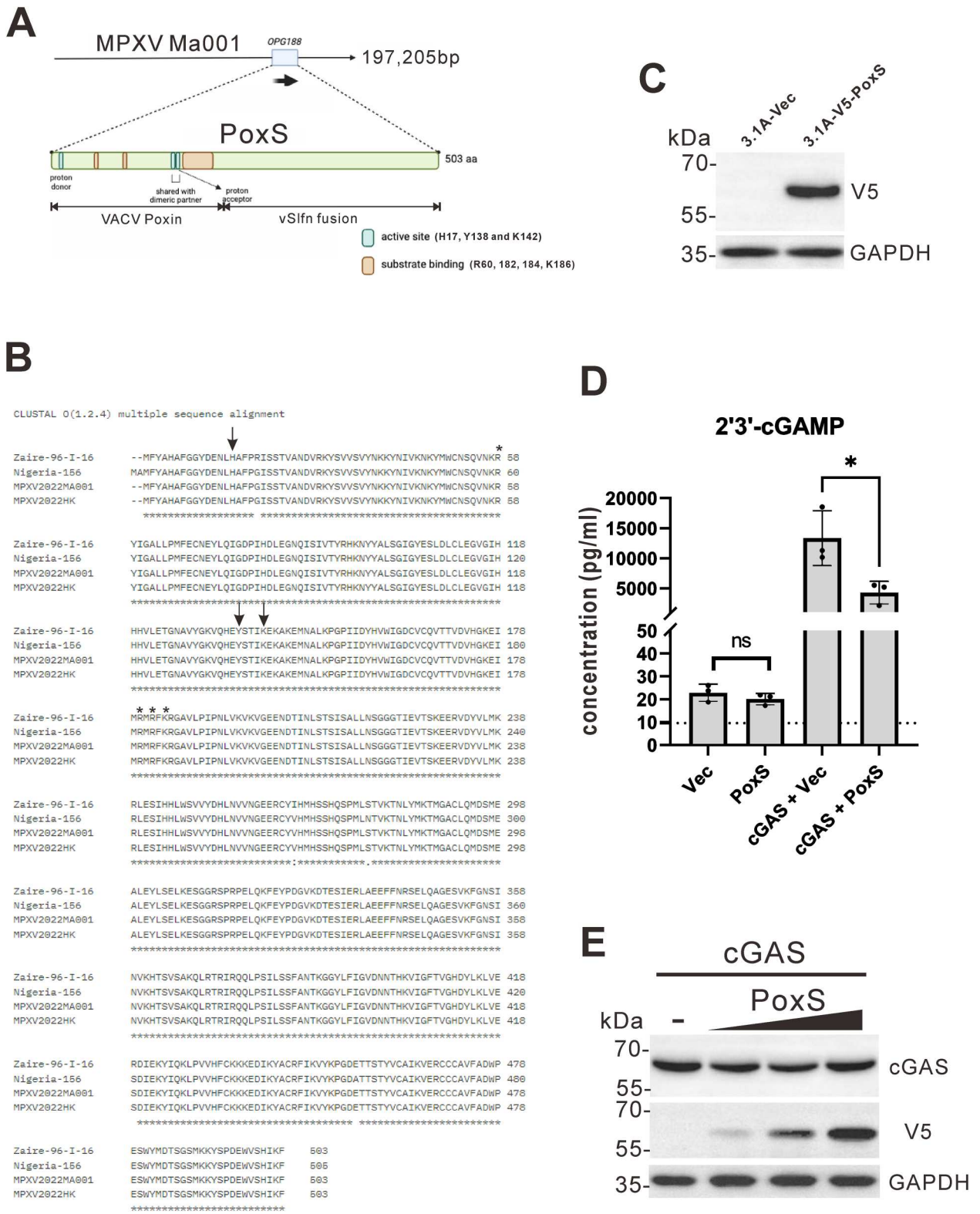

Figure 1. Diminution of cGAS-produced 2′3′-cGAMP when MPXV PoxS was expressed. (A) A diagram showing the details of MPXV PoxS gene (OPG188) of MPXV MA001. (B) Multiple sequence alignment of MPXV PoxS of clade I (Zaire-96-I-16, NC_003310), clade IIA (Nigeria-156, KJ642615.1) and clade IIB (MA001, ON563414 and hMpxV/Hong Kong/HKU-220914-001/2022, GISAID accession no.: EPI_ISL_14945299). Arrows indicated the HYK catalytic triad. Asterisks indicated 2′3′-cGAMP binding sites. (C) HEK293T cells were transfected with pcDNA™3.1/V5-His A empty vector or pcDNA™3.1/V5-His A-MPXV-PoxS. Cellular protein was extracted at 48 hours post-transfection. MPXV-PoxS-V5-6xHis fusion protein was detected by Western blotting using anti-V5 antibody. GAPDH served as loading control. (D) Cellular 2′3′-cGAMP of HEK293T cells transfected without (vector control) or with cGAS and/or MPXV PoxS expression constructs was extracted with M-PER lysis buffer. 2′3′-cGAMP was detected by ELISA. Experiments were performed in triplicates. (E) HEK293T cells were transfected with pcDNA™3.1/V5-His A empty vector or increasing dose of pcDNA™3.1/V5-His A-MPXV-PoxS together with cGAS expression construct. cGAS, MPXV PoxS and GAPDH proteins were detected by Western blotting. An unpaired student *t*-test was performed to compare sample groups for statistical significance. *P* value less than 0.05, 0.01 or 0.001 was defined as statistically significant (*), very significant (**) or extremely significant (***). Otherwise, the difference between sample groups was statistically not significant (ns).

primer sequences used for subcloning MPXV PoxS gene were 5′-TCGAGGGATC CACCATGTTT TACGCACACG CTTTCG (forward) and 5′-TCAGACTCGA GAAATTTTAT ATGTGACACC CATTCATCTG GAG (complementary sequence to MPXV PoxS was underlined). BamHI and XhoI restriction sites were used for subcloning. Expression plasmids pCAGEN-cGAS and pcDNA6-STING for human cGAS and STING have been previously described [33]. Expression plasmids for codon-optimized MPXV PoxS-eGFP, PoxS-4A-eGFP, and PoxS-Poxin-eGFP were made on eGFP-N1 backbone with the help of Suzhou Hongxun Biotechnologies. Expression constructs for STAT1 and STAT2 as well as reporter plasmids driven by IFNβ promoter, ISRE, and GAS were used as previously described [34,35].

2′3′-cGAMP was purchased from Invivogen (Cat. No.: tlrl-nacga23-02). Human IFNβ (Cat. No.: 11415) and IFNγ (Cat. No.: 300-02) recombinant proteins were purchased from PBL Assay Science and PeproTech, respectively and used as previously described [36].

Tissue culture and transfection

HEK293T, A549, and Vero-E6 cells were cultured as previously described [34,37]. NuLi-1 cells were purchased from American Type Culture Collection (ATCC) and cultured in DMEM with 10% fetal bovine serum and 50 U/mL penicillin–streptomycin. A549 and Vero-E6 cells were transfected with Lipofectamine 3000 (ThermoFisher). NuLi-1 cells were transfected with TransfeX (ATCC). HEK293T cells were transfected with GeneJuice (Novagene). For 2′3′-cGAMP transfection, lipofectamine 3000 was used.

Virus and infection experiment

MVA-BN (VR-1508) was purchased from ATCC. MVA-BN was propagated twice in BHK21 cells. In brief, confluent BHK21 cells were infected with diluted MVA-BN stock. On day 4, extensive cytopathic effects were observed. The infected cells were subjected to three freeze–thaw cycles as described [38]. Then, cell debris was pelleted by centrifugation at 2000×g for 10 min. The supernatant was aliquoted and stored at – 80°C. For infection experiment, 100 µl of MVA-BN of the 2nd passage was used to infect NuLi-1 cells. RNA and DNA samples of MVA- infected or mock infected NuLi-1 cells were collected and extracted respectively with RNeasy mini kit plus (Qiagen) and Quick-DNA Microprep Kit (Zymo Research).

All procedures with the use of live MPXV were conducted at Biosafety Level 3 containment facility in Block T of Queen Mary Hospital. The first isolate of MPXV in Hong Kong (hMpxV/Hong Kong/HKU-220914-001/2022) was fully sequenced [32]. The isolate was propagated in Vero-E6 cells. In brief, MPXV viral stock was used to infect confluent Vero-E6 cells. At 24 hours after infection, media containing the parental MPXV were replaced with serum-free DMEM. On day 7, extensive cytopathic effects were observed. The vessels containing the infected cells and supernatant were subjected to three freeze–thaw cycles as described and following Biosafety Level 3 procedures [38]. Then, cell debris was pelleted at 2000×g for 10 min. The supernatant was aliquoted and stored at –80°C.

The MPXV stocks were quantified with standard plaque assay. In brief, MPXV stocks were diluted 10-fold serially. Confluent Vero-E6 cells were then infected with the diluted viruses. After one day, infectious media were removed. The infected cells were then overlaid with 1% agarose in DMEM. At 4 days post-infection, 4% paraformaldehyde was added to inactivate infectious MPXV and to fix the infected cells. At 24 hours after fixation, the agarose overlay was carefully removed. 0.5% crystal violet solution in 10% methanol was used to stain the cells. The number of plaques were calculated and the concentration of the MPXV stock was determined.

For qPCR quantification of MPXV genome, viral genomes in virus-containing samples were extracted with AVL lysis buffer. Viral genomes were purified with the QIAamp Viral Kit (Qiagen) following the manufacturer's instruction. The purified viral genome was directly assayed with qPCR analysis with TB Green Premix Ex Taq II provided by Takara Bio. The primer sequences to amplify the MPXV genome were 5′-TACGGAACGG GACTATGGAC (forward) and 5′-ATCGAGCGCG GCTACTATAA for MPXV TK, 5′-TACCGTCCCA AAACATGGAT (forward) and 5′-CAAACGTGCA ATTTGTGGAC for MPXV A10L, 5′-CTCCATCATT TCCGCATTCT (forward) and 5′-TGTCCATCCC CCACCTAATA for MPXV A27L, as well as 5′-CTGGCGGCTA GAATGGCATA (forward) and 5′-GACACTCTG GCAGCCGAAA T for MPVX I4L.

Protein analysis, immunostaining and reporter assays

Anti-V5 was purchased from ThermoFisher Scientific. Anti-pSTAT1 S727 (D3B7, Cat. No.: 62390) and anti-cGAS (D1D3G) was from Cell signalling Technology. Anti-pSTAT2 Y690 (Cat. No.: AF2890) was from R&D Systems. Anti-STAT2 (A-7, Cat. No.: sc-1688), anti-STAT1, anti-JAK1, anti-Myc and anti-GAPDH were from Santa Cruz Biotechnology. Anti-Flag (M2) was from Sigma-Aldrich. 4′,6-Diamidino-2-phenylindole (DAPI) was purchased from ThermoFisher

Scientific. Dual luciferase reporter assay, immunofluorescent staining, co-immunoprecipitation, SDS-PAGE and Western blot analysis were conducted as previously described [34,35].

RNA assays

Cellular RNA was collected with RLT lysis buffer followed by RNA purification with RNeasy mini kit plus (Qiagen) using the manufacturer's protocol. RNA amount and quality of the RNA samples were assayed with NanoDrop Microvolume Spectrophotometers. 1 μg RNA sample was used for reverse transcription with the PrimeScript RT Reagent Kit with gDNA Eraser provided by Takara Bio. RT primer mix containing oligo-dT and random hexamer provided by the kit was used. The cDNA samples were subjected to qPCR analysis with TB Green Premix Ex Taq II provided by Takara Bio. The qPCR primer sequences were 5′-AGGACAGGAT GAACTTTGAC (forward) and 5′-TGATAGACAT TAGCCAGGAG for human IFNβ, 5′-GATGGCCACC AGTTCCAGAA (forward) and 5′-CTCTGTTCCC AAGCAGCAGA for human IFNα4, 5′-TGCTGGTGAC TTTGGTGCTA (forward) and 5′-CTCACCTGGA GAAGCCTCAG for human IFNλ, 5′-CAAGCTCAAG AGCCTCATCC (forward) and 5′-TGGGCTGTGT TGAAATGTGT for human OAS-1, 5′-GCAACCATCC ATAGACCTGA C (forward) and 5′-AATAGTGCCA TTGGTACGTG AAT for human SAMD9, 5′-GAAACAGGAG CACTCAATCT CA (forward) and 5′-CAGCCTTACT GGTGATTTTC ACA for human SAMD9L, as well as 5′-AAGATCCGAG AAGAATACCC TGA (forward) and 5′-CTACCAACTG ATGGACGGAG A for human β-tubulin.

2′ 3′-cGAMP ELISA

Around 1×10^6 HEK293T cells were lysed in 0.5 mL M-PER lysis buffer (ThermoFisher) in the presence of 1× EDTA-free protease inhibitor cocktail (Roche). Cells were lysed at 4°C for 10 min with agitation. Insoluble cell debris was pelleted by centrifugation at 21,500×g for 10 min. The supernatant was then used for quantification of 2′3′-cGAMP content with the 2′3′-cGAMP competition ELISA kit provided by Cayman Chemical. The manufacturer's instructions were followed. Briefly, cellular 2′3′-cGAMP, the 2′3′-cGAMP-HRP probe and the anti-2′3′-cGAMP antibody were mixed and loaded onto the mouse anti-rabbit IgG-coated ELISA stripes provided by the kit. After 2 hours incubation at room temperature with continuous rotational mixing, the ELISA stripes were washed with the 1× wash buffer provided by the kit. The amount of the bound 2′3′-cGAMP HRP probe was stained with the TMB solution. The mixture was quenched with the stop solution. The ELISA stripes were read against 450 nm absorbance with spectrophotometer. The absorbance of samples or standards (from 0 to 100,000 pg/mL) were subtracted with the absorbance of the non-specific binding control that had no anti-2′3′-cGAMP antibody added, giving the corrected absorbance B. The corrected absorbance of the 0 ng/mL sample was the maximal binding B_0. A standard curve plotting $\%B/B_0$ against $\log_{10}$ 2′3′-cGAMP concentration was generated. The 2′3′-cGAMP concentration of samples were extrapolated.

Colocalization analysis

Selected confocal images acquired through LSM980 with Airyscan super-resolution function were analysed through BIOP JACoP plug-in of Fiji software [39]. Pearson colocalization coefficient (PCC) was obtained from the scatterplot of pixels of two different channels. The scatterplots are shown in Figures S6, S7 and S10C, D. The area of each pixel of the super-resolution confocal images was 35 nm × 35 nm. PCC equals +1 means absolute linear correlation and colocalization of pixels. PCC equals – 1 means absolute inverse correlation of pixels and 0 means no correlation of pixels. Three to ten GFP positive cells were selected for calculation of PCC.

Statistical analysis

All experiments were performed at least in biological triplicates. The statistical significance was assessed with unpaired Student *T*-tests or one-way ANOVA by Graphpad Prism. Only when the *P* value or the adjusted *P* value comparing the sample groups reached less than 0.05 (i.e. above 95% confidence interval) then a change was defined to be statistically significant. Otherwise, we followed the theory of null hypothesis. (n.s.: $P > 0.05$, *: $P < 0.05$, **: $P < 0.01$, ***: $P < 0.001$, ****: $P < 0.0001$).

Results

Decline of cGAS-produced 2′3′-cGAMP upon expression of MPXV PoxS

Poxin and vSlfn are expressed from the OPG188 gene of the MPXV of the 2022 outbreak as a fusion protein abbreviated as PoxS (Figure 1(A)). PoxS of MPXV 2022 is highly similar to its counterpart in clade I (Zaire-96-I-16) and clade IIA (Nigeria-156) viruses (Figure 1(B)). MPXV PoxS of MA001 is identical to that in the Hong Kong isolate. The HYK catalytic triad (H17, Y138 and K142) for the nuclease activity against 2′3′-cGAMP are conserved and intact for MPXV PoxS [22,31]. The functional 2′3′-cGAMP binding sites R60, R182, R184 and K186 are also

conserved and intact (Figure 1(B)). In this study, PoxS from MPXV 2022 was used throughout and was named MPXV PoxS for simplicity.

We first sought to determine whether MPXV PoxS might counteract cGAS-dependent production of 2′3′-cGAMP. We confirmed the expression of MPXV PoxS from HEK293T transfected with the expression construct in the backbone of pcDNA™3.1/V5-His A (Figure 1(C)). Then, MPXV PoxS was expressed in HEK293T cells with and without enforced expression of cGAS (Figure 1(D)). HEK293T cells are defective in cGAS and STING function with very low expression of cGAS and no expression of STING [40,41]. Without overexpression of cGAS, cellular 2′3′-cGAMP was detectable in HEK293T cells but the level was very low and close to the lowest detection limit (9.6 pg/mL) of the competitive ELISA. Enforced expression of cGAS robustly elevated 2′3′-cGAMP level to about 13.3 ng/mL (19.7 μM). Expression of MPXV PoxS decreased the cGAS-induced 2′3′-cGAMP level to 4 ng/mL (5.93 μM). Expression of MPXV PoxS also decreased basal 2′3′-cGAMP from 22.9 pg/mL to 20.1 pg/mL, but the change did not reach statistically significant range. Plausibly, the low amount of basal 2′3′-cGAMP might render it suboptimally accessible to MPXV PoxS. Finally, MPXV PoxS expression had minimal effect on protein stability of cGAS (Figure 1(E)). In short, MPXV PoxS significantly diminished intact 2′3′-cGAMP generated by cGAS in mammalian cells.

No suppression of cGAS-STING-mediated IFN production by MPXV PoxS

STING protein is very sensitive in the detection of nanomolar 2′3′-cGAMP over bacterial cyclic dinucleotides for type I IFN production [42]. In addition, STING protein does not bind linear Gp(2′−5′)Ap(3′), which is the direct hydrolytic product of 2′3′-cGAMP generated by poxin [22]. With this in mind, we set out to determine if MPXV PoxS might suppress type I IFN response induced by activated STING. STING was activated either by cGAS overexpression or co-treatment with external 2′3′-cGAMP in the absence and presence of MPXV PoxS in HEK293T cells. To our surprise, MPXV PoxS did not suppress either cGAS- or 2′3′-cGAMP-mediated transcriptional activation of IFNβ promoter in STING-reconstituted HEK293T cells (Figure 2(A)). To verify the result of the reporter assay, mRNAs of types I and III IFNs, including IFNβ, IFNα4 and IFNλ, were detected with RT-qPCR. Consistently, MPXV PoxS did not mitigate either type I or type III IFN transcription induced by cGAS + STING reconstitution in HEK293T cells (Figure 2(B)). OAS-1 is an ISG, the expression of which is purely dependent on type I IFN signalling and JAK/STAT activation but not IRF3 [43,44]. cGAS + STING reconstitution promoted OAS-1 expression (Figure 2(B)). Interestingly, MPXV PoxS significantly blunted cGAS-STING-mediated OAS-1 expression by 50%. Therefore, MPXV PoxS did not suppress cGAS- or 2′3′-cGAMP-induced type I IFN production.

To obtain a more physiologically relevant condition, endogenous antiviral response was assessed in NuLi-1 cells which were immortalized human bronchiolar cells expressing intact and functional cGAS and STING innate immune sensing pathway [45]. MVA infection of NuLi1 can induce type I IFN response [45]. Consistently, MVA infection triggered IFNβ and OAS1 expression in infected NuLi-1 cells (Figure 2(C)). MVA infectivity was comparable between vector control and PoxS-expressing cells. Again, we failed to detect the suppression of MVA-induced IFNβ expression by MPXV PoxS (Figure 2(C)). Instead, MVA-induced OAS1 expression was dampened by MPXV PoxS. We also detected SAMD9, which is another ISG with potent antiviral function against poxvirus infection [46]. We found that MPXV PoxS suppressed SAMD9 expression induced by MVA infection (Figure 2(C)).

Hence, although MPXV PoxS possessed 2′3′-cGAMP nuclease activity, it did not suppress IFN production induced by 2′3′-cGAMP + STING, cGAS + STING or MVA infection. Instead, MPXV PoxS might act more downstream of the IFN response to exert a suppressive effect on ISG expression.

Suppression of basal and type I IFN-induced ISG expression by MPXV PoxS

ISG expression is regulated by IFN signalling [47]. To verify if MPXV PoxS might suppress type I or type II IFN signalling, the activity of human IFNβ or IFNγ recombinant protein was assessed in HEK293T cells using luciferase reporter driven by ISRE and GAS, respectively. We found that MPXV PoxS suppressed IFNβ-induced ISRE reporter activity by about 50% (Figure 3(A)). MPXV PoxS also suppressed basal ISRE reporter activity without addition of IFNβ. In contrast, MPXV PoxS did not mitigate IFNγ-induced GAS reporter activity (Figure 3(A)). To validate the results from reporter assays, ISG mRNA levels were detected by RT-qPCR in the presence and absence of human IFNβ in HEK293T cells. Two representative ISGs known as OAS1 and SAMD9, both of which have been shown to be critical in restricting poxvirus replication [48–50], were analysed. It was found that MPXV PoxS dampened IFNβ-induced OAS1 and SAMD9 expression by 22.4% and 39.1%, respectively (Figure 3(B)). We have also detected SAMD9L, which is another ISG and a paralog to SAMD9 also capable of suppressing poxvirus replication [49]. We found that IFNβ-induced SAMD9L was decreased

upon expression of MPXV-PoxS by about 50% (Figure 3(B)). Interestingly, MPXV PoxS also suppressed basal SAMD9 expression (Figure 3(B)). Basal mRNA expression of OAS-1 and SAMD9L was undetectable in HEK293T cells. Similar findings were also obtained in HEK293T and human lung epithelial A549 cells with additional ISGs including ISG15, ISG56, IFIT3 and MxA (Figures S1 and S2).

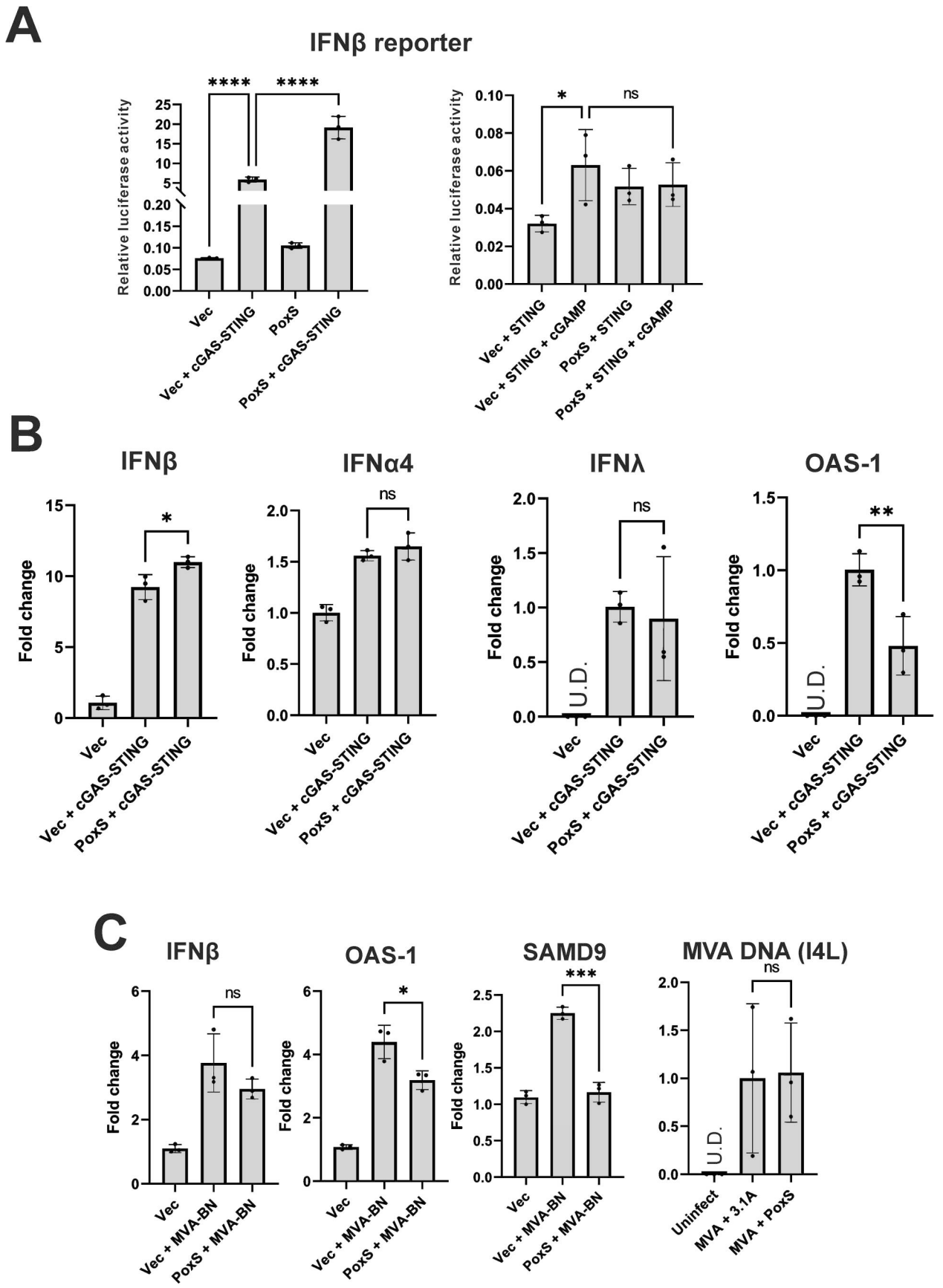

Therefore, MPXV PoxS specifically suppressed type I but not type II IFN signalling. Moreover, MPXV PoxS suppressed basal ISRE activity and ISG expression.

Suppression of type I IFN-induced STAT2 phosphorylation by MPXV PoxS

Type I IFN signalling is initiated with type I IFN binding to the IFNAR1 and IFNAR2, in which the respectively pre-associated TYK2 and JAK1 are activated [51]. TYK2 and JAK1 phosphorylate STAT2 and STAT1 which form heterodimer and further recruit IRF9 to form ISGF3. ISGF3 translocates to the nucleus for transcriptional activation of ISGs through ISRE. STAT2 Y690 phosphorylation is generated by activated IFNAR1/2-TYK2/JAK1 complex to promote STAT2 interaction with STAT1 [52]. Activated IFNAR1/2-TYK2/JAK1 also phosphorylates STAT1 at S701 and S727 sites [53,54].

To interrogate if MPXV perturbed STAT1 and STAT2 phosphorylation induced by type I IFNs, Western blot analysis was performed. We found that MPXV PoxS expression potently suppressed STAT2 Y690 phosphorylation in the presence of IFNβ, but suppression of STAT1 S727 phosphorylation by MPXV PoxS was not observed in the same setting (Figure 3(C,D)). Therefore, MPXV PoxS specifically targeted STAT2 but not STAT1 or the upstream receptor-associated tyrosine kinases of IFNAR for suppression of type I IFN signalling.

Interaction of MPXV PoxS with STAT2 and their colocalization to cytosolic clusters

We next interrogated whether MPXV PoxS might differentially interact with STAT1 and STAT2. Co-immunoprecipitation was performed in HEK293T cells expressing PoxS and STAT1 or STAT2 proteins. In the anti-V5 precipitate that contains PoxS-V5 protein, STAT2-Flag was detected but STAT1-Myc was absent (Figure 3(E)). Thus, consistent with its impact on STAT2 but not STAT1 (Figure 3(C,D)), MPXV PoxS preferentially interacts with STAT2.

To further delineate the mechanism of action for MPXV PoxS, we constructed two mutants. They were the PoxS-4A mutant, in which the HYK catalytic triad (H17, Y138 and K142) and the functional 2′3′-cGAMP binding site (R184) had been mutated to alanine [22], and the Poxin only mutant named PoxS-Poxin, which only contained the poxin gene (amino acid 1-214) corresponding to vaccinia virus poxin (Figure 1(A) and Figure S3A). eGFP was C-terminally fused with the MPXV PoxS, PoxS-4A and PoxS-Poxin. The expression constructs were codon optimized for human cell expression. Their subcellular localization and expression level in A549 (Figure S4A) and HEK293T cells (Figure S4B) were checked by fluorescent microscopy. Expression of MPXV PoxS and its mutants gave similar eGFP fluorescent signal in both HEK293T and A549 cells when compared with GFP control. Interestingly, MPXV PoxS formed very distinct cytosolic clusters in A549 cells (Figure S4A). In HEK293T cells, MPXV PoxS was partly diffusive and clustered in the cytosol (Figure S4B). Deletion of vSlfn fusion subverted the cytosolic clustering pattern and rendered PoxS-Poxin to diffuse both in the nucleus and the cytosol (Figure S4A,B), although some speckle-like entities were still observed for PoxS-Poxin in A549 cells (Figure S4A). PoxS-4A showed a similar clustering pattern compared with MPXV PoxS (Figure S4A,B). This suggested that MPXV PoxS clustering in the cytosol might be driven by the vSlfn fusion but the active site of the 2′3′-cGAMP nuclease was not required.

As MPXV PoxS interacted with and suppressed phosphorylation of STAT2 but not STAT1 (Figure 3(C, E)), we reasoned that MPXV PoxS might colocalize specifically with STAT2. Confocal microscopy was performed in A549 cells expressing MPXV PoxS (Figure 4(A)). We found that MPXV PoxS colocalized and clustered with a significant subset of STAT2 outside the nucleus (Figure 4(A)). Such pattern was easily observed in multiple views with mean Pearson's correlation coefficient (PCC)

← **Figure 2.** Impact of MPXV PoxS on cGAS-STING-mediated type I IFN production. (A) Impact on cGAS-STING-induced IFNβ promoter activity. IFNβ promoter activity was stimulated by either cGAS + STING (left) or STING + cGAMP (right) in HEK293T cells transfected with vector control (Vec) or with MPXV PoxS expression construct. IFNβ promoter-driven firefly luciferase plasmid and the SV40 early constitutively active promoter-driven Renilla luciferase plasmid served as reporter. Cells were collected at 48 hours for dual luciferase assay. At 24 hours after transfection, cells were further stimulated with lipofectamine3000 reagent alone or with 1 μg/mL 2′3′-cGAMP (lipofectamine3000-2′3′-cGAMP complex). At 48 hours, cells were harvested for luciferase assay through measurement of LAR-II and S&G substrates using luminometer. (B) HEK293T cells were transfected with vector control (Vec) or with cGAS + STING plasmids together with vector control (Vec) or MPXV PoxS expression construct. At 48 hours, cellular RNA was extracted for RT-qPCR analysis of the mRNA expression levels of IFNβ, IFNα4, IFNλ and OAS-1 genes. (C) NuLi-1 cells were transfected with vector control (Vec) or with MPXV PoxS construct. At 24 hours, cells were infected with MVA-BN (VR-1508). At another 24 hours, cellular RNA was extracted for RT-qPCR analysis of the mRNA expression levels of IFNβ, OAS1 and SAMD9 gene. Human β-tubulin mRNA was used as internal control for RT-qPCR analysis. Moreover, cellular DNA was collected for qPCR quantification of MVA viral DNA at I4L gene. Experiments were performed in biological triplicates. Statistical analysis was performed as in Figure 1.

equalling 0.480 (Figure 5(A,D); Figures S5–S8). Z-stack 3D confocal imaging showed that MPXV PoxS formed cytosolic perinuclear clusters with STAT2 (Figure 4(B); Videos S1-S6). Nevertheless, MPXV PoxS did not cluster or colocalize with STAT1 (Figure 4(A), Figure S9A). Since STAT2 Y690 phosphorylation was suppressed by MPXV PoxS (Figure 3(C)), we asked if MPXV PoxS might cluster with the upstream receptor-associated tyrosine kinase of IFNAR1. It was found that MPXV PoxS did not colocalize or cluster with IFNAR1-associated kinase JAK1 (Figure 4(A), Figure S9B). The mean PCCs of PoxS/STAT1 and PoxS/JAK1 were respectively 0.354 and 0.302 which were lower than that of PoxS/

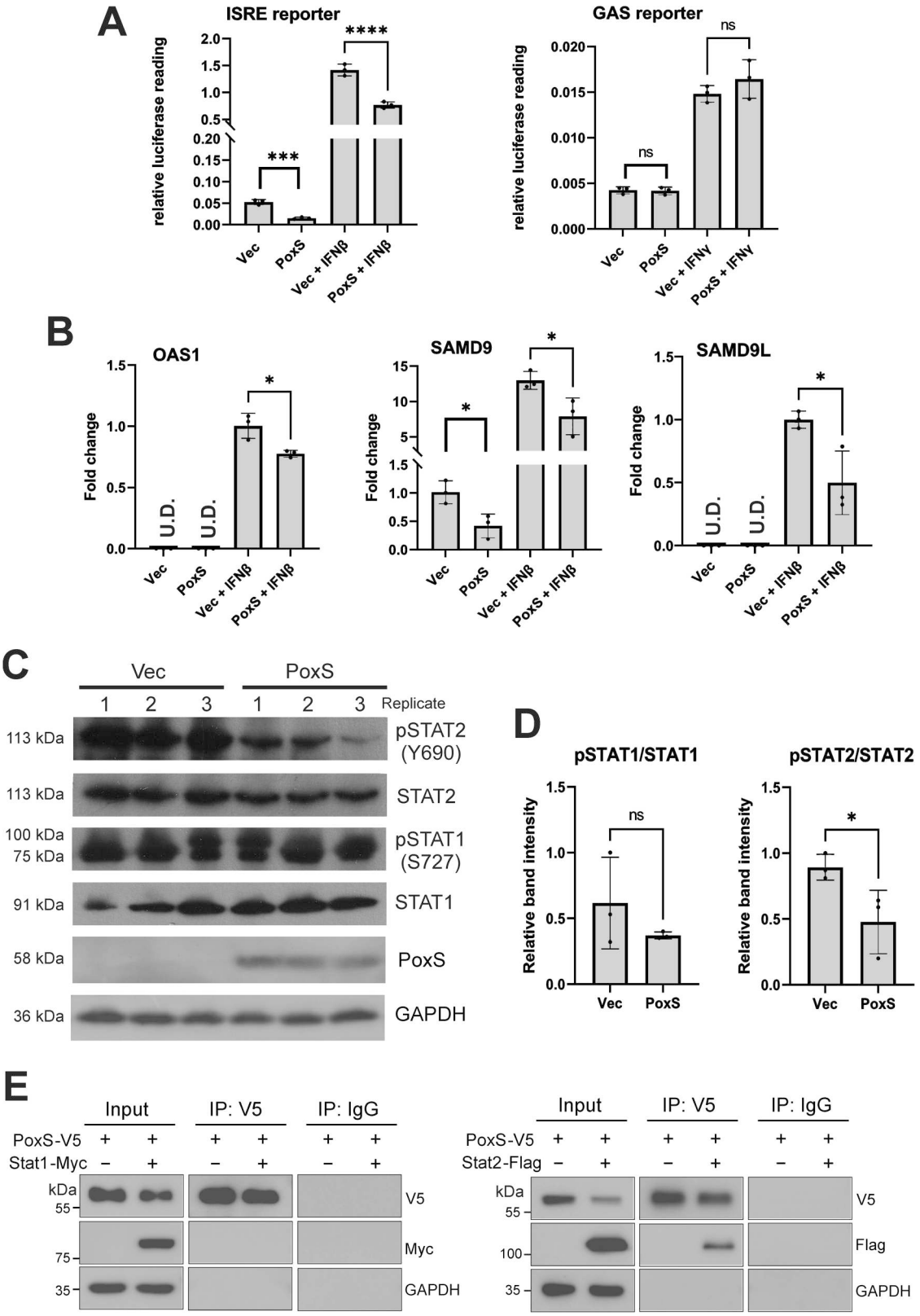

STAT2 which was 0.480 (Figure 5(D) vs Figure S9C). Therefore, our results showed that MPXV PoxS specifically targeted STAT2 and retained it in the cytosolic clusters.

Requirement of intact nuclease active site and vSfln fusion for cytosolic sequestration of STAT2 by MPXV PoxS

Furthermore, we compared the subcellular localization of STAT2 in the presence of MPXV PoxS, PoxS-4A or PoxS-Poxin in A549 cells. Although PoxS-4A formed cytosolic clusters like MPXV PoxS (Figure S4), STAT2 did not colocalized or clustered with PoxS-4A (Figure 5(B), Views 1-3). PoxS-Poxin was more diffusive than MPXV PoxS and PoxS-4A (Figure 5(C), Views 1-3). However, PoxS-Poxin occasionally formed disperse speckle-like structure that still colocalized with STAT2 (Figure 5(C), View 3; Figure S8C, View 5 and 6). The PCC of STAT2 with PoxS-4A and PoxS-Poxin were 0.188 and 0.473, respectively (Figure 5(D)). Images used for the colocalization analysis were summarized in Figure S5A. The pixel scatterplots can be found in Figure S6. PCC of PoxS-4A/STAT2 was significantly less than that of PoxS-WT/STAT2 or PoxS-Poxin/STAT2. More importantly, STAT2 localized to the nucleus in cells expressing PoxS-4A (Figure 5(B), Figure S8B, arrowed). Likewise, nuclear localization of STAT2 was observed in cells expressing PoxS-Poxin (Figure 5(C), Figure S8C, arrowed). However, STAT2 was seldom localized to the nucleus when MPXV PoxS was expressed (Figure 4(A,B), Figure 5(A) and Figure S8(A)) PCC of STAT2 with DAPI staining was calculated (Figure 5(E)). Images used for the colocalization analysis and the pixel scatterplots of STAT2/DAPI were summarized in respectively Figures S5B and S7. Consistently, PoxS WT significantly reduced PCC of STAT2/DAPI compared with PoxS-4A (Figure 5(E)). In contrast, PoxS-Poxin did not significantly decrease PCC of STAT2/DAPI compared with PoxS-4A although the mean value was slightly reduced. This suggested that MPXV PoxS might sequester STAT2 at the cytosolic cluster to prevent its nuclear translocation. The sequestration required both the intact active site of 2′3′-cGAMP nuclease and the vSfln fusion.

Requirement of intact nuclease active site and vSfln fusion for subversion of antiviral response by MPXV PoxS

We next investigated the functional outcomes of the expression of MPXV PoxS, PoxS-4A or PoxS-Poxin that had different properties in sequestering STAT2. STAT2 supports not only constitutive ISG expression by forming STAT2-IRF9 or unphosphorylated ISGF3, but also type I IFN-induced ISG expression by forming phosphorylated ISGF3 [55,56]. To shed light on this, ISG expression was assayed in NuLi-1 cells expressing MPXV PoxS, PoxS-4A or PoxS-Poxin. The three representative ISGs, namely OAS1, SAMD9 and SAMD9L, which have been shown to be critical in restricting poxvirus replication [48–50], were chosen in our assay. MPXV-PoxS markedly diminished OAS-1, SAMD9 and SAMD9L expression both in the presence and absence of IFNβ treatment in NuLi-1 cells (Figure 6(A)). PoxS-4A or PoxS-Poxin did not suppress OAS-1 and SAMD9 expression without IFNβ treatment. In the presence of IFNβ, PoxS-4A and PoxS-Poxin still had a slight suppressive effect on SAMD9 and SAMD9L but not OAS-1 expression. This effect of PoxS-4A or PoxS-Poxin was much weaker than that of MPXV PoxS. Hence, we confirmed that PoxS-4A and PoxS-Poxin not only lost the ability to sequester STAT2 in the cytosol, but also lost the functional suppressive effect on ISG expression.

Finally, the efficiency of IFNβ in suppressing MPXV replication was tested in Vero-E6 cells expressing eGFP, MPXV PoxS, PoxS-4A or PoxS-Poxin.

← **Figure 3.** Suppression of type I IFN signalling by MPXV PoxS and its interaction with STAT2. (A) Dual luciferase reporter assay was performed in HEK293T cells to assess the ISRE- or GAS-driven promoter activity of different treatment groups as indicated. HEK293T cells were transfected with vector control (Vec) or with MPXV PoxS expression construct together with the reporter constructs. Renilla luciferase plasmid under the control of constitutively active SV40 early promoter was used as internal control. At 24 hours, cells were either mock treated or treated with 1000 U/mL IFNβ or 100 ng/mL IFNγ recombinant protein. At 48 hours, cells were harvested for detection of the luciferase activity through LAR-II and S&G substrates on luminometer. (B) HEK293T cells were transfected and treated with or without IFNβ as in (A) but without reporter constructs. At 48 hours, cellular RNA was extracted for RT-qPCR analysis of the mRNA expression levels of OAS1, SAMD9 and SAMD9L genes. Human β-tubulin mRNA served as the internal control. U.D.: undetected. (C) HEK293T cells were transfected and treated with IFNβ as in (A) but without reporter constructs. After 24 hours of treatment with IFNβ, cellular protein was extracted in RIPA lysis buffer and assayed through SDS-PAGE and Western blotting with anti-pSTAT2 (Y690), anti-STAT2, anti-pSTAT1 (S727), anti-STAT1, anti-V5 (PoxS) and GAPDH. Experiments were performed in biological triplicates. (D) Densitometry of p-STAT1, p-STAT2, STAT1 and STAT2 bands in (C) were quantified with ImageJ software. Relative band intensity of p-STAT1/STAT1 and p-STAT2/STAT2 was calculated. For the STAT1 doublet, the upper band should be doubly phosphorylated form of STAT1 at p-S727 and p-Y701 [54]. The lower band should be STAT1 with single p-S727. The combination of both represented the total level of p-S727 STAT1. The quantification in the bar chart was based on total p-S727 STAT1. Statistical analysis was performed as in Figure 1. (E) Co-immunoprecipitation. HEK293T cells were transfected with PoxS-V5 and STAT2-Flag or STAT-1-Myc expression plasmids. Cell lysates were collected by 1% NP40 buffer and immunoprecipitation was performed with the indicated antibodies. Mouse IgG (Santa Cruz sc-2025) was used as negative control.

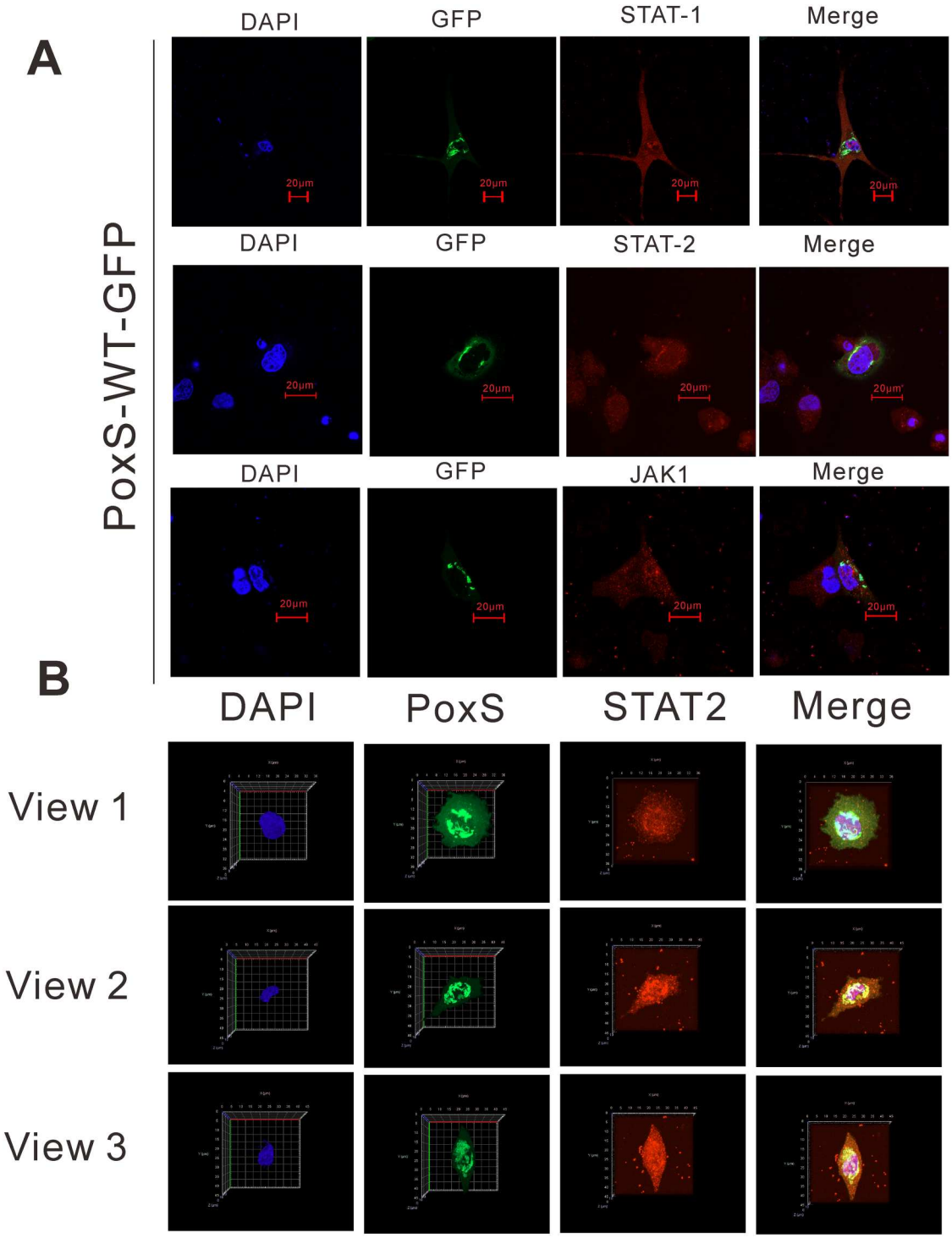

Figure 4. Colocalization of MPXV PoxS with STAT2. A549 cells were transfected with expression construct for eGFP-tagged MPXV PoxS. At 24 hours, cells were fixed with PBS-buffered 4% paraformaldehyde and permeabilized with PBS-buffered 0.2% Triton X100. (A) Cells were stained with anti-STAT1, anti-STAT2 or anti-JAK1 followed by secondary antibody with rhodamine conjugate and DAPI staining. Cells were visualized on confocal microscope LSM980 with Airyscan function. (B) Cells expressing MPXV PoxS and stained with STAT2 were subjected to Z-stack confocal imaging through LSM980. Z-stack images were 0.129 µm apart with 50% layer-overlap. A total of 210–211 slices were captured. 3D images were generated by Zen 3.3 software. Three bird views of the 3D images were shown.

IFNβ treatment reduced MPXV DNA replication in Vero-E6 cells expressing eGFP as detected by qPCR targeting viral genome at viral thymidine kinase (TK), A10L, A27L, and I4L regions (Figure 6(B)). IFNβ treatment also significantly reduced the infectious titre of replicating MPXV (Figure 6(C)).

We found that MPXV PoxS expression markedly increased viral DNA replication (Figure 6(B)) and infectious titre of MPXV (Figure 6(C)) in the presence of IFNβ. PoxS-4A did not significantly rescue IFNβ-dependent suppression of MPXV DNA replication (Figure 6(B)). The increase in infectious

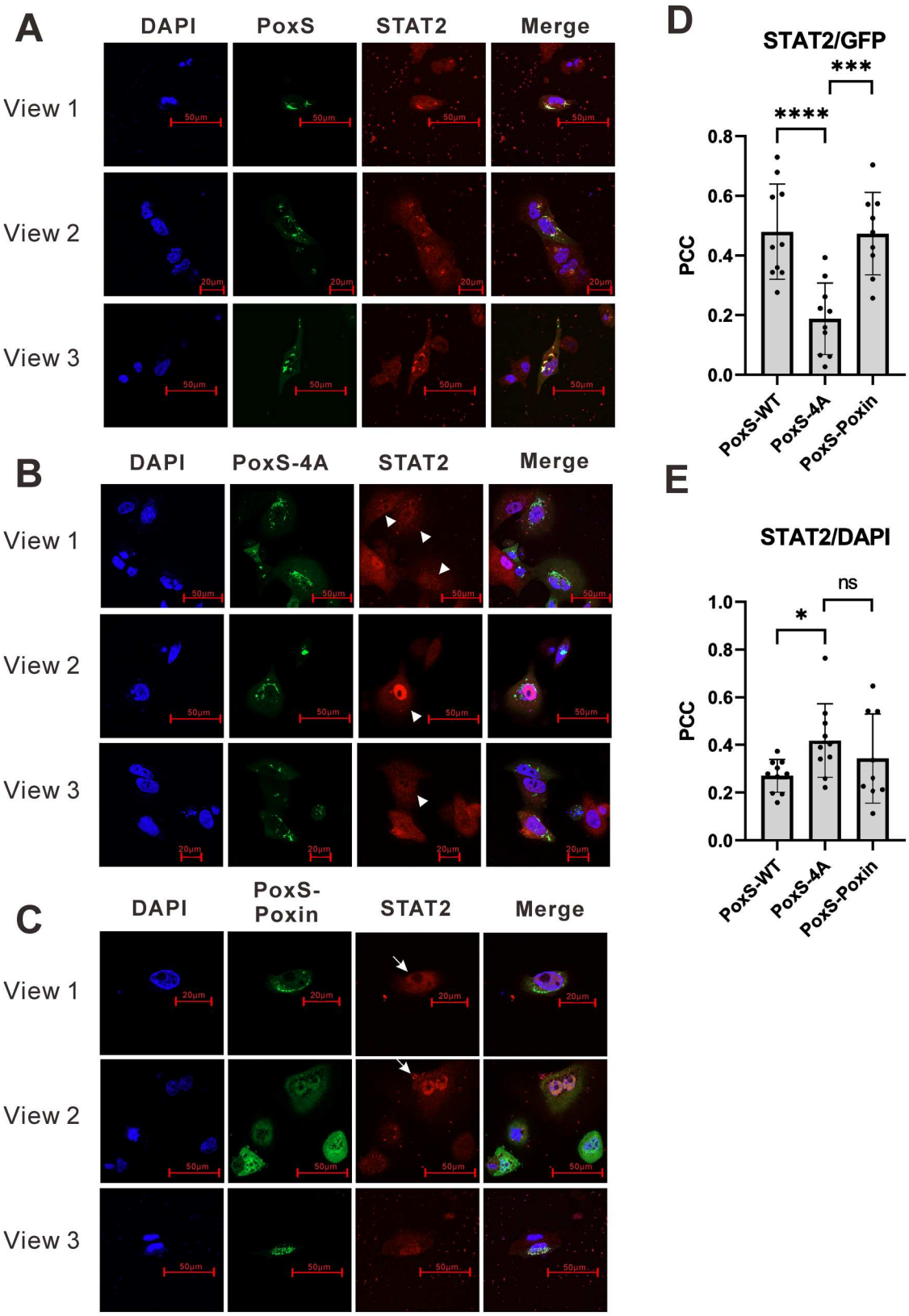

Figure 5. Requirement of vSlfn fusion and the active site of 2′3′-cGAMP nuclease of MPXV PoxS for STAT2 sequestration. A549 cells were transfected with expression constructs for eGFP-tagged MPXV-PoxS (A), eGFP-tagged PoxS-4A (B) and eGFP-tagged PoxS-Poxin (C). Cells were fixed and stained as in Figure 4. Three representative views were shown. Arrows indicated nuclear localization of STAT2 in eGFP-positive cells. (D) eGFP signal of A549 cells expressing eGFP-tagged MPXV-PoxS ($n = 10$), eGFP-tagged PoxS-4A ($n = 10$) or eGFP-tagged PoxS-Poxin ($n = 9$) were analysed for colocalization with STAT2. The degree of colocalization was expressed as the value of Pearson's colocalization correlation (PCC) of pixels of eGFP and STAT2. (E) Similar to (D), the colocalization of DAPI and STAT2 was quantified and expressed as PCC. One-way ANOVA was used to evaluate statistical significance between independent sample groups. Adjusted *P* value less than 0.05 was defined as being statistically significant.

MPXV titre ascribed to PoxS-4A was milder than that attributed to MPXV PoxS upon treatment with IFNβ (Figure 6(C)). To our surprise, PoxS-Poxin was fully competent in conferring resistance to IFNβ treatment in MPXV-infected cells, resembling MPXV PoxS (Figure 6(B, C)). Hence, MPXV PoxS conferred resistance to IFNβ during MPXV replication (Figure 6(B, C)). Although

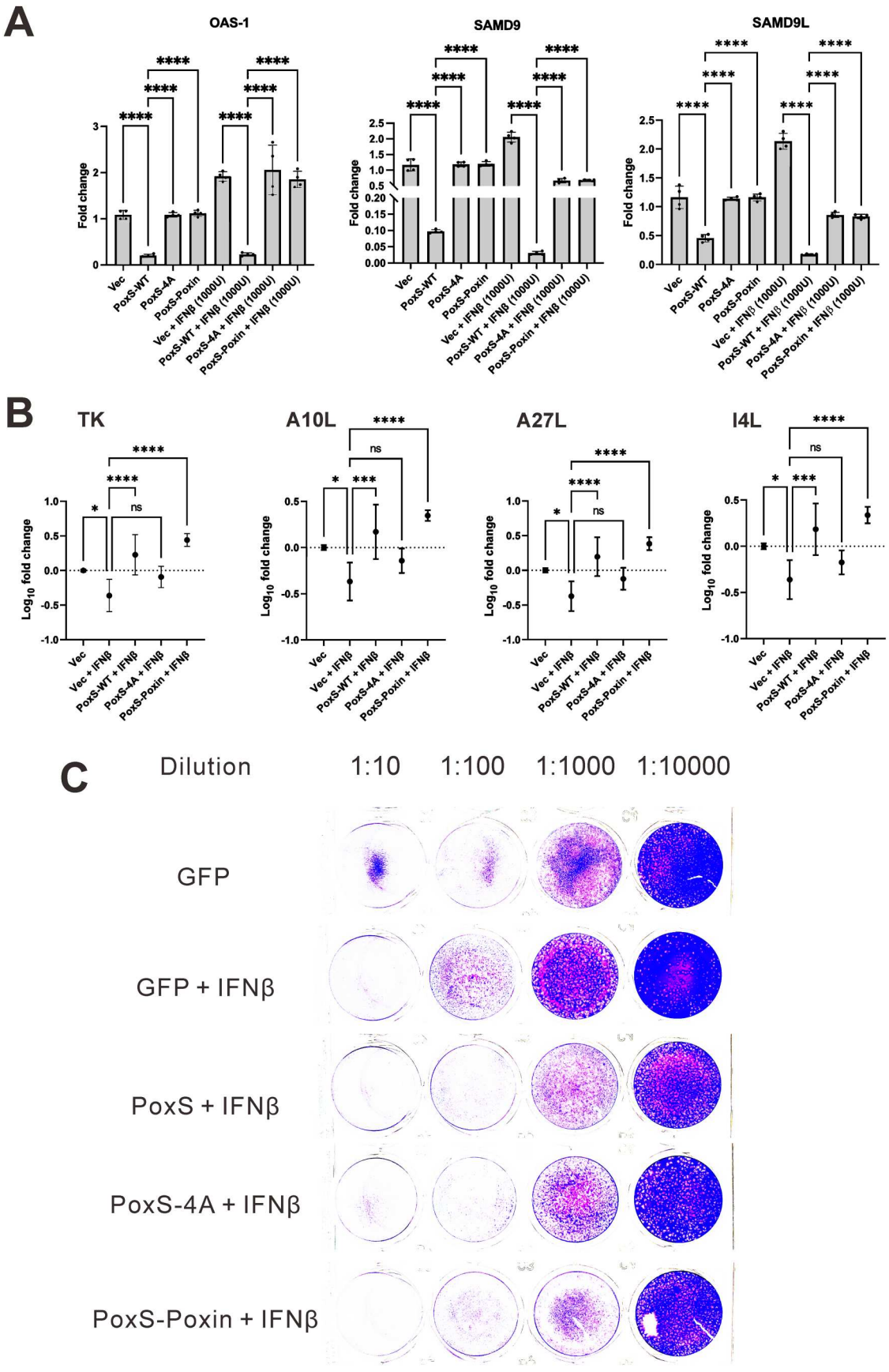

PoxS-4A and PoxS-Poxin failed to suppress ISG expression (Figure 6(A)), they still exerted a mild alleviative effect on IFNβ-dependent suppression of MPXV replication.

Discussion

Our primary goal was to determine if MPXV PoxS suppressed cGAS-STING-mediated type I IFN production by hydrolysing 2′3′-cGAMP. Surprisingly, although it blunted cGAS-dependent 2′3′-cGAMP production (Figure 1(D)), MPXV PoxS did not suppress cGAS-STING-induced type I IFN production (Figure 2). We have examined three types of stimuli for activation of cGAS-STING-mediated type I IFN production. This included cGAS overexpression (Figure 2(A,B)), extrinsic 2′3′-cGAMP administration (Figure 2(A)) and MVA infection in NuLi-1 cells expressing endogenous cGAS and STING (Figure 2(C)). MPXV PoxS failed to suppress type I IFN production induced by any of the three stimuli. One possibility is that MPXV PoxS is not sufficiently efficient in hydrolysing 2′3′-cGAMP generated by cGAS to a level that STING protein is no longer responsive to propagate IFN production. STING protein is very sensitive to 2′3′-cGAMP with a lower response limit of 5 nM [42]. cGAS overexpression generated 19.7 μM 2′3′-cGAMP (Figure 1(D)). MPXV PoxS can only reduce 2′3′-cGAMP to the level of 5.93 μM, which is still a thousand times more than the lower limit to activate STING. Moreover, MPXV PoxS did not significantly suppress MVA-induced type I IFN production in NuLi-1 cells (Figure 2(C)), suggesting that MPXV PoxS was not sufficiently efficient in counteracting endogenous cGAS and STING signalling. Considering this together with our observation that MPXV PoxS was recruited to the cytosolic clusters (Figure S4), the restricted subcellular localization of MPXV PoxS might have reduced its efficiency in hydrolysing cytosolic 2′3′-cGAMP produced by cGAS. Vaccinia virus poxin, which lacks vSlfn fusion and is cytosolic, might therefore be more effective in suppressing cGAS-STING-mediated type I IFN production, although that is still context-specific [22]. PoxS might even slightly promote IFNβ promoter activity and IFNβ expression induced by cGAS-STING or STING (Figure 2(A), vec + cGAS-STING versus PoxS + cGAS-STING and vec + STING versus PoxS + STING), although the pattern was not consistent for all IFN inducers such as cGAMP + STING and MVA (Figures 2(A–C)). We confirmed that PoxS did not affect cGAS protein stability (Figure 1(E)). One possibility is that PoxS suppresses one of the negative feedback inhibitors of IFN signalling [57] triggered by cGAS-STING overexpression in HEK293T cells. With less inhibitors, IFN production might be enhanced. Future investigations are required to clarify this.

We noted that the suppressive effect of PoxS on IFN signalling in HEK293T cells was generally less dramatic than in lung epithelial cells (Figures 3(B) vs 6(A)). Cytosolic clustering of PoxS was more prominently observed in lung epithelial cells than in HEK293T cells (Figures S4A vs S4B). It is possible that STAT2 sequestration by PoxS in HEK293T cells was not as effective as in lung epithelial cells, although the underlying mechanisms for the potential cell type-specific effect require future investigations. The target tissues and cells of MPXV *in vivo* might be more complicated than we expected. MPXV infection in skin and kidney organoids has recently been reported [58,59]. Thus, it will be of interest to further analyse MPXV infection in different types of organoids and primary human cells including immune cells. Transcriptomic analysis of ISG induction by MPXV and its PoxS protein will also shed light on their global effects on host defence.

MPXV PoxS cannot suppress MVA-induced type I IFN production (Figure 2(C)), indicating the inability of MPXV PoxS to counteract MVA-dependent activation of endogenous STING in NuLi-1 cells. This raises questions about the physiological roles of MPXV PoxS during poxviral infection. MPXV PoxS is apparently not capable of preventing the first wave of poxviral induction of type I IFN production.

← **Figure 6.** Requirement of vSlfn fusion and the active site of 2′3′-cGAMP nuclease of MPXV PoxS for suppression of ISG expression in transfected cells and type I IFN antiviral response in MPXV-infected cells. (A) NuLi-1 cells were transfected with the expression construct for eGFP (vec), MPXV PoxS-eGFP (PoxS-WT), PoxS-4A-eGFP or PoxS-Poxin-eGFP. At 24 hours, cells were either mock treated or treated with 1000 U/mL IFNβ. At 48 hours, cellular RNA was extracted for RT-qPCR analysis of the mRNA expression levels of OAS1, SAMD9 and SAMD9L genes. Human β-tubulin mRNA was used as the internal control. (B, C) Vero-E6 cells were transfected with the expression construct for eGFP (Vec), MPXV PoxS-eGFP (PoxS-WT), PoxS-4A-eGFP or PoxS-Poxin-eGFP. At 24 hours, cells were infected with hMpxV/Hong Kong/HKU-220914-001/2022 at MOI = 0.00035. At 48 hours, cells were either mock treated or treated with 1000 U/mL IFNβ. At 96 hours, infectious MPXV was obtained by three freeze-thaw cycles. (B) Viral DNA was extracted from the freeze-thaw lysate and quantitated with qPCR targeting viral TK, A10L, A27L and I4L genes. (C) Infectious viral quantities of the freeze-thaw lysates were detected and estimated by standard plaque assay. Experiments were performed in biological triplicates. Statistical analysis was performed with one-way Anova. For (B), One-way ANOVA was performed to compare all samples with Vec + IFNβ group. Adjusted *P* value less than 0.05 was defined as being statistically significant. Otherwise, the difference between sample groups and Vec + IFNβ group was statistically not significant (ns).

However, it appears to be a functional 2′3′-cGAMP hydrolase (Figure 1(D)) that could still prevent overproduction of 2′3′-cGAMP. Further investigations including accurate and sensitive analysis of 2′3′-cGAMP might help to define the conditions under which MPXV PoxS might make a difference. Particularly, it will be of interest to clarify whether MPXV PoxS can suppress type I IFN production when 2′3′-cGAMP concentration becomes limiting.

MPXV PoxS efficiently suppressed ISRE activity and ISG expression by targeting STAT2. We found that MPXV suppressed ISG expression induced by cGAS-STING activation (Figure 2(B)), MVA infection (Figure 2(C)) and IFNβ treatment (Figures 3(B) and 6(A)). MPXV PoxS suppressed ISG expression even in the absence of any stimuli Figures 3(B), 6(A), S1 and S2. Consistently, MPXV PoxS suppressed ISRE activity in the presence and absence of IFNβ treatment (Figure 3B). STAT2 is the key to constitutive and type I IFN- induced ISG expression [51,52]. We found that MPXV PoxS suppressed IFNβ-induced STAT2 phosphorylation (Figure 3(C, D)) and nuclear translocation (Figures 4 and 5(A, E)). Interestingly, the interaction between MPXV PoxS and STAT2 required the active

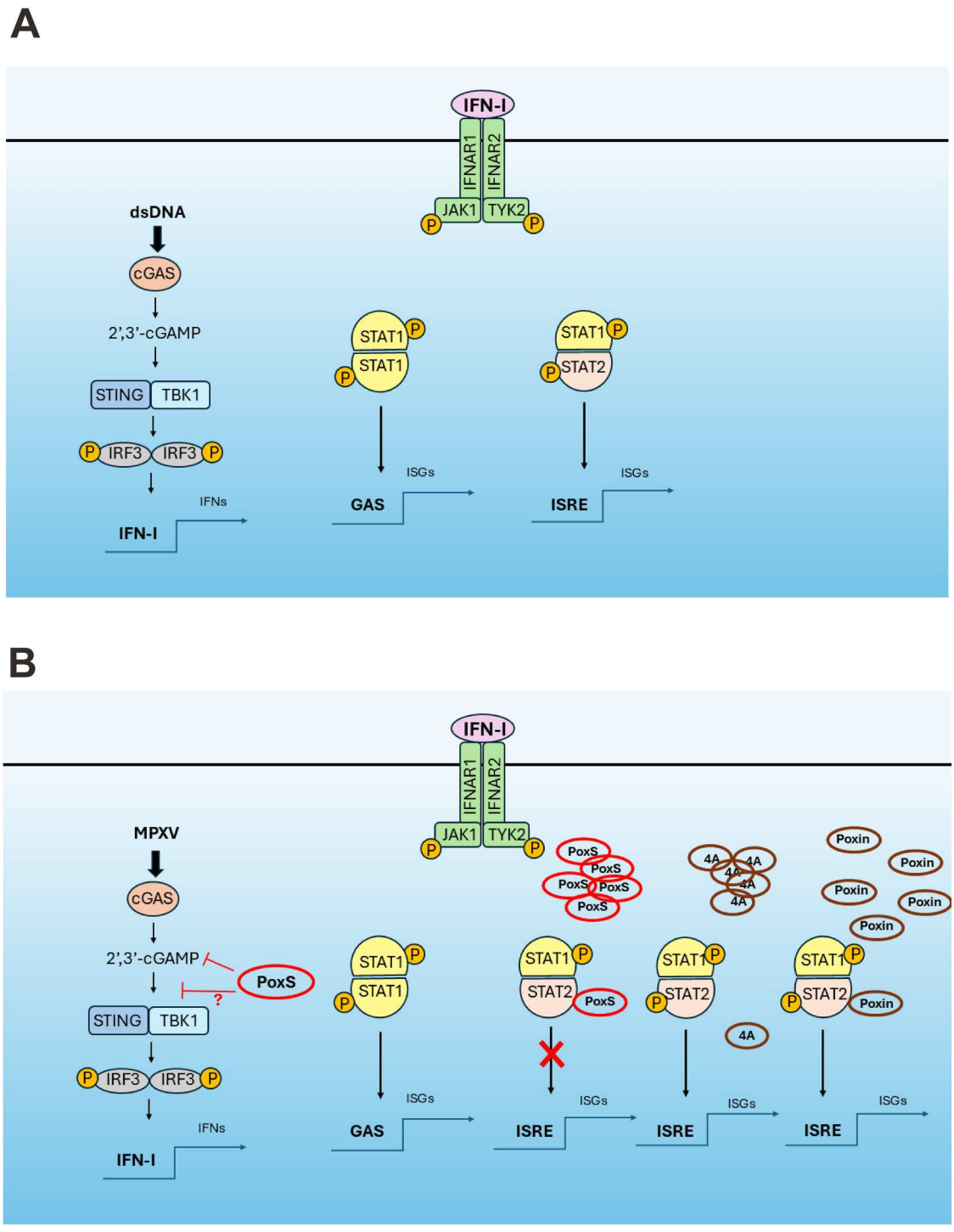

site of 2′3′-cGAMP nuclease (Figure 5(D)). Although vSlfn fusion was required for cytosolic clustering (Figure 5(C), Figure S4 and Figure S8C), it was not required for MPXV PoxS-STAT2 interaction (Figure 5(D)). However, MPXV PoxS-mediated ISG suppression was abolished in PoxS-4A or PoxS-Poxin mutant (Figure 6(A)). This suggests that both STAT2 binding and cytosolic clustering are required for the inhibition of STAT2 function. The sequestration of STAT2 in the cytosolic clusters might have prevented STAT2 from being phosphorylated by IFNAR1/2-TYK2-JAK1 upon type I IFN stimulation. A proposed model for MPXV PoxS in IFN antagonism is illustrated in Figure 7. Our findings are generally consistent with recent results obtained from the analysis of poxin-deficient vaccinia virus and PoxS-deficient ectromelia virus [60].

In the presence of endogenous MPXV PoxS in infected cells, PoxS-4A conferred milder protection than that ascribed to MPXV PoxS but PoxS-Poxin worked equally well as MPXV PoxS to reverse IFNβ suppression of MPXV replication (Figure 6(B,C)). Probably, the overexpressed PoxS-4A, which cannot bind directly to STAT2, can still modestly confer IFNβ resistance by associating with the endogenous MPXV PoxS through vSlfn-vSlfn interaction, which is a typical property of schlafen proteins having the schlafen core domain [61]. The limited amount of endogenous MPXV PoxS, which can only absorb STAT2 to certain extent, restricted the enhancement given by PoxS-4A. On the other hand, PoxS-Poxin can directly recruit and absorb STAT2 (Figure 5(D)). Although PoxS-Poxin did not form cytosolic clusters and cannot function efficiently in suppressing ISG expression when it was expressed alone (Figure 6(A)), PoxS-Poxin might associate with endogenous MPXV PoxS through poxin-poxin interaction during MPXV infection [23]. Possibly, the limited amount of endogenous MPXV PoxS could form cytosolic clustering "seed" to recruit more PoxS-Poxin and the associated STAT2 onto the cytosolic clusters. Therefore, PoxS-Poxin overexpression worked as efficiently as that of MPXV PoxS in antagonizing IFNβ suppression of MPXV replication.

Why is the catalytic active site of the 2′3′-cGAMP nuclease of MPXV PoxS required for STAT2 sequestration by MPXV PoxS? It is possible that 2′3′-cGAMP changed the structure or intermolecular property of MPXV PoxS that 2′3′-cGAMP-bound MPXV PoxS is more favourable in recognizing STAT2. With a mutation in the major 2′3′-cGAMP binding site of R184, PoxS-4A cannot interact with 2′3′-cGAMP. Therefore, PoxS-4A could not maintain the structure or intermolecular property required for interaction with STAT2. Alternatively, a recent study by Wang et al. on STAT2 and STING provided some hint to the property of STAT2 [62]. In that study, STAT2 was found to be an inhibitor to control STING activation. Importantly, STAT2 was found to bind directly to STING only in the presence of 2′3′-cGAMP. STAT2-STING binding occurred in the endoplasmic reticulum (ER) and prevented active STING from correctly translocating away from ER. It is unclear whether STING might perturb the function of STAT2 through this interaction. However, the study suggests that STAT2 can interact and sequester 2′3′-cGAMP-bound STING but not apo-STING in ER. Plausibly, STAT2 might interact with 2′3′-cGAMP or with 2′3′-cGAMP-bound proteins. Further investigations are required to clarify whether 2′3′-cGAMP could facilitate MPXV PoxS-STAT2 interaction.

STAT2 sequestration to cytosolic clusters by MPXV PoxS significantly reduced nuclear STAT2 (Figures 4 and 5(A,E)), type I IFN-induced STAT2 phosphorylation (Figure 3(C, D)) and ISG expression (Figure 6(A)). vSlfn fusion is the key for cytosolic

← **Figure 7.** Schematic diagram of the proposed model for MPXV PoxS-mediated IFN antagonism. (A) The cGAS-STING pathway and type-I IFN signalling. Briefly, cGAS senses and binds dsDNA in the cytoplasm, which facilitates the production of 2′3′-cGAMP. In turn, 2′3′-cGAMP activates STING which triggers phosphorylation and dimerization of IRF3 through TBK1. The activated IRF3 homodimer translocates into the nucleus and stimulates type I IFN production. Secreted type I IFNs then bind to the type I IFN receptor complex on the cell membrane. This activates the JAK-STAT pathway. STAT1 is phosphorylated, self-dimerizes, binds and transactivates GAS promoter for ISG expression. STAT2 is phosphorylated and forms heterodimers with STAT1. The activated STAT1/2 complex further recruits IRF9 to form ISGF3, that finally binds and transactivates ISRE promoter for ISG expression. (B) MPXV PoxS-mediated perturbation of 2′3′-cGAMP and type I IFN signalling. Upon MPXV infection, viral DNA activates cGAS. With 2′3′-cGAMP hydrolyase activity, PoxS counteracts 2′3′-cGAMP synthesized by cGAS. Whether PoxS-mediated 2′3′-cGAMP suppression would affect type I IFN production through STING might be context-specific. On the other hand, PoxS downregulates interferon-stimulated gene expression by sequestering and inhibiting STAT2. Y690 phosphorylation of STAT2 is downregulated by PoxS. Cytosolic clustering of PoxS with STAT2 is necessary for this process which requires vSlfn domain and the intact 2′3′-cGAMP hydrolase active site. PoxS without vSlfn domain is unable to form cytosolic clusters. Catalytically dead mutant, PoxS-4A, that had alanine substitutions in its 2′3′-cGAMP hydrolase active site still forms cytosolic clusters but cannot interact with STAT2. In contrast, Poxin binds well with STAT2. Both Poxin and PoxS-4A fail to suppress type I IFN signalling compared with the WT PoxS. This suggests that intact PoxS of MPXV is required for the suppression of STAT2 and IFN signalling. Together, these findings suggest: (i) PoxS downregulates 2′3′-cGAMP level and may affect cGAS-STING-mediated antiviral response depending on the context (e.g. the resulting 2′3′-cGAMP concentration and the strength of STING protein response). (ii) PoxS suppresses STAT2-mediated IFN signalling. (iii) The potential role of vSfln for mediating cytosolic clustering of the PoxS protein. and (iv) The integrity of the active site of 2′3′-cGAMP hydrolase is necessary for PoxS to interact with STAT2. The ancestral conformational structure of the Poxin domain might be required for STAT2 interaction.

cluster formation of MPXV PoxS (Figure S4). PoxS-Poxin without vSlfn did not effectively suppress ISG expression (Figure 6(A)). vSlfn belongs to the type I schlafen family. However, type I schlafen and camelpox PoxS (i.e. vSlfn in the paper) were found to be diffusive in the cytosol [63–65]. Interestingly, when we compared the amino acid sequence of camelpox PoxS (GenBank accession number: AY009089) and MPXV PoxS, remarkable divergence was seen in the vSlfn fusion (215-503 amino acids) versus the poxin domain (1-214 amino acids) (Figure S3B). Plausibly, the cytosolic clustering property is subtype-specific to MPXV PoxS and specifically requires the vSlfn fusion which is conserved in MPXV (Figure 1(B)).

Acknowledgements

We thank the State Key Laboratory of Emerging Infectious Diseases, the Faculty Central Facilities, Centre for PanorOmic Sciences (CPOS), and the Department of Pathology for facility and technical support; and members of the Jin group for critical reading of the manuscript.

Disclosure statement

No potential conflict of interest was reported by the author(s).

Funding

The study was supported by Hong Kong Research Grants Council (17127019 and 17127423), Hong Kong Health and Medical Research Fund (CID-HKU1-9) and InnoHK (CVVT).

Author contributions

Study design: Pearl Chan, Zi-Wei Ye, Pak-Hin Hinson Cheung, Dong-Yan Jin; Experiments and data analysis: Pearl Chan, Zi-Wei Ye, Pak-Hin Hinson Cheung, Wenlong Zhao; Tools and techniques: Chon Phin Ong, Xiaoyu Sun; Study supervision and fund acquisition: Pak-Hin Hinson Cheung, Dong-Yan Jin; Manuscript writing: Pearl Chan, Pak-Hin Hinson Cheung, Dong-Yan Jin.

Data availability statement

The original data of this study will be made available upon reasonable request to the corresponding authors.

ORCID

Pearl Chan http://orcid.org/0000-0002-9979-516X
Zi-Wei Ye http://orcid.org/0000-0002-6446-4299
Pak-Hin Hinson Cheung http://orcid.org/0000-0003-3682-7571
Dong-Yan Jin http://orcid.org/0000-0002-2778-3530

References

[1] Boehm E, Summermatter K, Kaiser L. Orthopox viruses: is the threat growing? Clin Microbiol Infect. 2024;30:883–887. doi:10.1016/j.cmi.2024.02.011
[2] Mitjà O, Ogoina D, Titanji BK, et al. Monkeypox. Lancet. 2023;401:60–74. doi:10.1016/S0140-6736(22)02075-X
[3] Silva NIO, de Oliveira JS, Kroon EG, et al. Here, there, and everywhere: The wide host range and geographic distribution of zoonotic orthopoxviruses. Viruses. 2020;13:43. doi:10.3390/v13010043
[4] Rimoin AW, Mulembakani PM, Johnston SC, et al. Major increase in human monkeypox incidence 30 years after smallpox vaccination campaigns cease in the Democratic Republic of Congo. Proc Natl Acad Sci USA. 2010;107:16262–16267. doi:10.1073/pnas.1005769107
[5] Masirika LM, Udahemuka JC, Schuele L, et al. Ongoing mpox outbreak in Kamituga, South Kivu province, associated with monkeypox virus of a novel clade I sub-lineage, Democratic Republic of the Congo, 2024. Euro Surveill. 2024;29:2400106. doi:10.2807/1560-7917.ES.2024.29.11.2400106
[6] Vakaniaki EH, Kacita C, Kinganda-Lusamaki E, et al. Sustained human outbreak of a new MPXV clade I lineage in eastern Democratic Republic of the Congo. Nature Med. 2024;30:2791–2795. doi:10.1038/s41591-024-03130-3
[7] Pan D, Nazareth J, Sze S, et al. Transmission of monkeypox/mpox virus: A narrative review of environmental, viral, host, and population factors in relation to the 2022 international outbreak. J Med Virol. 2023;95:e28534. doi:10.1002/jmv.28534
[8] Beeson A, Styczynski A, Hutson CL, et al. Mpox respiratory transmission: the state of the evidence. Lancet Microbe. 2023;4:e277–e283. doi:10.1016/S2666-5247(23)00034-4
[9] Grandvaux N, tenOever BR, Servant MJ, et al. The interferon antiviral response: from viral invasion to evasion. Curr Opin Infect Dis. 2002;15:259–267. doi:10.1097/00001432-200206000-00008
[10] Smith GL, Talbot-Cooper C, Lu Y. How does vaccinia virus interfere with interferon? Adv Virus Res. 2018;100:355–378. doi:10.1016/bs.aivir.2018.01.003
[11] Dai P, Wang W, Cao H, et al. Modified vaccinia virus Ankara triggers type I IFN production in murine conventional dendritic cells via a cGAS/STING-mediated cytosolic DNA-sensing pathway. PLoS Pathog. 2014;10:e1003989. doi:10.1371/journal.ppat.1003989
[12] Waibler Z, Anzaghe M, Frenz T, et al. Vaccinia virus-mediated inhibition of type I interferon responses is a multifactorial process involving the soluble type I interferon receptor B18 and intracellular components. J Virol. 2009;83:1563–1571. doi:10.1128/JVI.01617-08
[13] Unterholzner L, Sumner RP, Baran M, et al. Vaccinia virus protein C6 is a virulence factor that binds TBK-1 adaptor proteins and inhibits activation of IRF3 and IRF7. PLoS Pathog. 2011;7:e1002247. doi:10.1371/journal.ppat.1002247
[14] Stuart JH, Sumner RP, Lu Y, et al. Vaccinia virus protein C6 inhibits type I IFN signalling in the nucleus and binds to the transactivation domain of STAT2. PLoS Pathog. 2016;12:e1005955. doi:10.1371/journal.ppat.1005955

[15] Zhao Y, Lu Y, Richardson S, et al. TRIM5α restricts poxviruses and is antagonized by CypA and the viral protein C6. Nature. 2023;620:873–880. doi:10.1038/s41586-023-06401-0
[16] Meade N, Toreev HK, Chakrabarty RP, et al. The poxvirus F17 protein counteracts mitochondrially orchestrated antiviral responses. Nat Commun. 2023;14:7889. doi:10.1038/s41467-023-43635-y
[17] Arndt WD, Cotsmire S, Trainor K, et al. Evasion of the innate immune type I interferon system by monkeypox virus. J Virol. 2015;89:10489–10499. doi:10.1128/JVI.00304-15
[18] Davies MV, Chang HW, Jacobs BL, et al. The E3L and K3L vaccinia virus gene products stimulate translation through inhibition of the double-stranded RNA-dependent protein kinase by different mechanisms. J Virol. 1993;67:1688–1692. doi:10.1128/jvi.67.3.1688-1692.1993
[19] Mohamed MR, Rahman MM, Lanchbury JS, et al. Proteomic screening of variola virus reveals a unique NF-(κB inhibitor that is highly conserved among pathogenic orthopoxviruses. Proc Natl Acad Sci USA. 2009;106:9045–9050. doi:10.1073/pnas.0900452106
[20] Shchelkunov SN, Totmenin AV, Safronov PF, et al. Analysis of the monkeypox virus genome. Virology. 2002;297:172–194. doi:10.1006/viro.2002.1446
[21] Weaver JR, Isaacs SN. Monkeypox virus and insights into its immunomodulatory proteins. Immunol Rev. 2008;225:96–113. doi:10.1111/j.1600-065X.2008.00691.x
[22] Eaglesham JB, Pan Y, Kupper TS, et al. Viral and metazoan poxins are cGAMP-specific nucleases that restrict cGAS-STING signalling. Nature. 2019;566:259–263. doi:10.1038/s41586-019-0928-6
[23] Eaglesham JB, McCarty KL, Kranzusch PJ. Structures of diverse poxin cGAMP nucleases reveal a widespread role for cGAS-STING evasion in host-pathogen conflict. Elife. 2020;9:e59753. doi:10.7554/eLife.59753
[24] Maluquer de Motes C. Poxvirus cGAMP nucleases: clues and mysteries from a stolen gene. PLoS Pathog. 2022;17:e1009372. doi:10.1371/journal.ppat.1009372
[25] Hernáez B, Alonso G, Georgana I, et al. Viral cGAMP nuclease reveals the essential role of DNA sensing in protection against acute lethal virus infection. Sci Adv. 2020;6:eabb4565. doi:10.1126/sciadv.abb4565
[26] Patel DJ, Yu Y, Xie W. cGAMP-activated cGAS-STING signaling: its bacterial origins and evolutionary adaptation by metazoans. Nat Struct Mol Biol. 2023;30:245–260. doi:10.1038/s41594-023-00933-9
[27] Li L, Yin Q, Kuss P, et al. Hydrolysis of 2'3'-cGAMP by ENPP1 and design of nonhydrolyzable analogs. Nat Chem Biol. 2014;10:1043–1048. doi:10.1038/nchembio.1661
[28] Yang N, Wang Y, Dai P, et al. Vaccinia E5 is a major inhibitor of the DNA sensor cGAS. Nat Commun. 2023;14:2898. doi:10.1038/s41467-023-38514-5
[29] Riederer S, Del Canizo A, Navas J, et al. Improving poxvirus-mediated antitumor immune responses by deleting viral cGAMP-specific nuclease. Cancer Gene Ther. 2023;30:1029–1039. doi:10.1038/s41417-023-00610-5
[30] Conrad SJ, Raza T, Peterson EA, et al. Myxoma virus lacking the host range determinant M062 stimulates cGAS-dependent type 1 interferon response and unique transcriptomic changes in human monocytes/macrophages. PLoS Pathog. 2022;18:e1010316. doi:10.1371/journal.ppat.1010316
[31] Duchoslav V, Boura E. Structure of monkeypox virus poxin: implications for drug design. Arch Virol. 2023;168:192. doi:10.1007/s00705-023-05824-4
[32] Chiu KH, Wong SC, Tam AR, et al. The first case of monkeypox in Hong Kong presenting as infectious mononucleosis-like syndrome. Emerg Microbes Infect. 2023;12:2146910. doi:10.1080/22221751.2022.2146910
[33] Lui WY, Bharti A, Wong NM, et al. Suppression of cGAS- and RIG-I-mediated innate immune signaling by Epstein-Barr virus deubiquitinase BPLF1. PLoS Pathog. 2023;19:e1011186. doi:10.1371/journal.ppat.1011186
[34] Cheung PHH, Lee TTW, Kew C, et al. Virus subtype-specific suppression of MAVS aggregation and activation by PB1-F2 protein of influenza A (H7N9) virus. PLoS Pathog. 2020;16:e1008611. doi:10.1371/journal.ppat.1008611
[35] Fung SY, Siu KL, Lin H, et al. SARS-CoV-2 NSP13 helicase suppresses interferon signaling by perturbing JAK1 phosphorylation of STAT1. Cell Biosci. 2022;12:36. doi:10.1186/s13578-022-00770-1
[36] Chaudhary V, Yuen KS, Chan JFW, et al. Selective activation of type II interferon signaling by Zika virus NS5 protein. J Virol. 2017;91:e00163-17. doi:10.1128/JVI.00163-17
[37] Siu KL, Chan CP, Chan C, et al. Severe acute respiratory syndrome coronavirus nucleocapsid protein does not modulate transcription of the human FGL2 gene. J Gen Virol. 2009;90:2107–2113. doi:10.1099/vir.0.009209-0
[38] Cotter CA, Earl PL, Wyatt LS, et al. Preparation of cell cultures and vaccinia virus stocks. Curr Protoc Protein Sci. 2017;89:5.12.1–5.12.18. doi:10.1002/cpps.34
[39] Bolte S, Cordelières FP. A guided tour into subcellular colocalization analysis in light microscopy. J Microsc. 2006;224:213–232. doi:10.1111/j.1365-2818.2006.01706.x
[40] Sun L, Wu J, Du F, et al. Cyclic GMP-AMP synthase is a cytosolic DNA sensor that activates the type I interferon pathway. Science. 2013;339:786–791. doi:10.1126/science.1232458
[41] Reus JB, Trivino-Soto GS, Wu LI, et al. SV40 large T antigen is not responsible for the loss of STING in 293 T cells but can inhibit cGAS-STING interferon induction. Viruses. 2020;12:137. doi:10.3390/v12020137
[42] Zhang X, Shi H, Wu J, et al. Cyclic GMP-AMP containing mixed phosphodiester linkages is an endogenous high-affinity ligand for STING. Mol Cell. 2013;51:226–235. doi:10.1016/j.molcel.2013.05.022
[43] Melchjorsen J, Kristiansen H, Christiansen R, et al. Differential regulation of the OASL and OAS1 genes in response to viral infections. J Interferon Cytokine Res. 2009;29:199–207. doi:10.1089/jir.2008.0050
[44] Kim A, Park JH, Lee MJ, et al. Interferon alpha and beta receptor 1 knockout in human embryonic kidney 293 cells enhances the production efficiency of proteins or adenoviral vectors related to type I interferons. Front Bioeng Biotechnol. 2023;11:1192291. doi:10.3389/fbioe.2023.1192291
[45] Massa D, Baran M, Bengoechea JA, et al. PYHIN1 regulates pro-inflammatory cytokine induction rather than innate immune DNA sensing in airway epithelial

cells. J Biol Chem. 2020;295:4438–4450. doi:10.1074/jbc.RA119.011400
[46] Tanaka M, Shimbo T, Kikuchi Y, et al. Sterile alpha motif containing domain 9 is involved in death signaling of malignant glioma treated with inactivated Sendai virus particle (HVJ-E) or type I interferon. Int J Cancer. 2010;126:1982–1991. doi:10.1002/ijc.24965
[47] Schoggins JW. Interferon-stimulated genes: what do they all do? Annu Rev Virol. 2019;6:567–584. doi:10.1146/annurev-virology-092818-015756
[48] Díaz-Guerra M, Rivas C, Esteban M. Inducible expression of the 2-5A synthetase/RNase L system results in inhibition of vaccinia virus replication. Virology. 1997;227:220–228. doi:10.1006/viro.1996.8294
[49] Meng X, Zhang F, Yan B, et al. A paralogous pair of mammalian host restriction factors form a critical host barrier against poxvirus infection. PLoS Pathog. 2018;14:e1006884. doi:10.1371/journal.ppat.1006884
[50] Zhang F, Ji Q, Chaturvedi J, et al. Human SAMD9 is a poxvirus-activatable anticodon nuclease inhibiting codon-specific protein synthesis. Sci Adv. 2023;9:eadh8502. doi:10.1126/sciadv.adh8502
[51] Platanias LC. Mechanisms of type-I- and type-II-interferon-mediated signalling. Nat Rev Immunol. 2005;5:375–386. doi:10.1038/nri1604
[52] Steen HC, Gamero AM. STAT2 phosphorylation and signaling. Jakstat. 2013;2:e25790.
[53] Tolomeo M, Cavalli A, Cascio A. STAT1 and its crucial role in the control of viral infections. Int J Mol Sci. 2022;23:4095. doi:10.3390/ijms23084095
[54] Nguyen H, Ramana CV, Bayes J, et al. Roles of phosphatidylinositol 3-kinase in interferon-γ-dependent phosphorylation of STAT1 on serine 727 and activation of gene expression. J Biol Chem. 2001;276:33361–33368. doi:10.1074/jbc.M105070200
[55] Blaszczyk K, Nowicka H, Kostyrko K, et al. The unique role of STAT2 in constitutive and IFN-induced transcription and antiviral responses. Cytokine Growth Factor Rev. 2016;29:71–81. doi:10.1016/j.cytogfr.2016.02.010
[56] Wang W, Yin Y, Xu L, et al. Unphosphorylated ISGF3 drives constitutive expression of interferon-stimulated genes to protect against viral infections. Sci Signal. 2017;10:eaah4248. doi:10.1126/scisignal.aah4248
[57] Arimoto KI, Miyauchi S, Stoner SA, et al. Negative regulation of type I IFN signaling. J Leukoc Biol. 2018;103:1099–1166. doi:10.1002/JLB.2MIR0817-342R
[58] Li P, Pachis ST, Xu G, et al. Mpox virus infection and drug treatment modelled in human skin organoids. Nat Microbiol. 2023;8:2067–2079. doi:10.1038/s41564-023-01489-6
[59] Li P, Du Z, Lamers MM, et al. Mpox virus infects and injures human kidney organoids, but responding to antiviral treatment. Cell Discov. 2023;9:34. doi:10.1038/s41421-023-00545-z
[60] Lant S, Hood AJM, Holley JA, et al. Poxin-deficient poxviruses are sensed by cGAS prior to genome replication. J Gen Virol. 2024;105:002036. doi:10.1099/jgv.0.002036
[61] Kim ET, Weitzman MD. Schlafens can put viruses to sleep. Viruses. 2022;14:442. doi:10.3390/v14020442
[62] Wang C, Nan J, Holvey-Bates E, et al. STAT2 hinders STING intracellular trafficking and reshapes its activation in response to DNA damage. Proc Natl Acad Sci USA. 2023;120:e2216953120. doi:10.1073/pnas.2216953120
[63] Gubser C, Goodbody R, Ecker A, et al. Camelpox virus encodes a schlafen-like protein that affects orthopoxvirus virulence. J Gen Virol. 2007;88:1667–1676. doi:10.1099/vir.0.82748-0
[64] Neumann B, Zhao L, Murphy K, et al. Subcellular localization of the Schlafen protein family. Biochem Biophys Res Commun. 2008;370:62–66. doi:10.1016/j.bbrc.2008.03.032
[65] Gubser C, Smith GL. The sequence of camelpox virus shows it is most closely related to variola virus, the cause of smallpox. J Gen Virol. 2002;83:855–872. doi:10.1099/0022-1317-83-4-855